

Nanoscale Glassification of Gold Substrates for Surface Plasmon Resonance Analysis of Protein Toxins with Supported Lipid Membranes

K. Scott Phillips, Jong-Ho Han, Marilyn Martinez, Zhuangzhi Wang, David Carter, and Quan Cheng*

Department of Chemistry, University of California, Riverside, California 92521

Surface plasmon resonance (SPR) spectroscopy, a powerful tool for biosensing and protein interaction analysis, is currently confined to gold substrates and the relevant surface chemistries involving dextran and functional thiols. Drawbacks of using self-assembled monolayers (SAMs) for SPR-related surface modification include limited stability, pinhole defects, bioincompatibility, and nonspecific protein adsorption. Here we report the development of stable nanometer-scale glass (silicate) layers on gold substrates for SPR analysis of protein toxins. The nanoscale silicate layers were built up with layer-by-layer deposition of poly(allylamine hydrochloride) and sodium silicate, followed by calcination at high temperature. The resulting silicate films have a thickness ranging from 2 to 15 nm and demonstrate outstanding stability in flow cell conditions. The use of these surfaces as a platform to construct supported bilayer membranes (SBMs) is demonstrated, and improved performance against protein adsorption on SBM-coated surfaces is quantified by SPR measurements. SBMs can be formed reproducibly on the silicate surface via vesicle fusion and quantitatively removed using injection of 5% Triton X-100 solution, generating a fresh surface for each test. Membrane properties such as lateral diffusion of the SBMs on the silicate films are characterized with photobleaching methods. Studies of protein binding with biotin/avidin and ganglioside/cholera toxin systems show detection limits lower than 1 $\mu\text{g/mL}$ (i.e., nanomolar range), and the response reproducibility is better than 7% RSD. The method reported here allows many assay techniques developed for glass surfaces to be transferred to label-free SPR analysis without the need for adaptation of protocols and time-consuming synthetic development of thiol-based materials and opens new avenues for developing novel bioanalytical technologies for protein analysis.

Surface plasmon resonance (SPR) spectroscopy is increasingly used as a unique and powerful analytical method for studies of biomolecular interactions and biosensing.^{1–4} The technique offers real-time and label-free detection with high sensitivity, allowing

for measurements of analyte concentration and binding kinetics as well as many applications of ligand fishing, epitope mapping, and molecular assembly tracking.⁵ Over the past 15 years, it has been applied to a wide range of research areas including amino acid sequencing,⁶ single nucleotide polymorphism analysis,⁷ protein conformation studies,^{8,9} and cell/ligand interactions.¹⁰ A recent development of SPR technology is the use of SPR imaging (SPRi) in high-throughput studies of enzyme kinetics, pharmaceutical screening, and DNA/protein and protein/protein interaction analysis.^{11–16} SPRi combines imaging analysis with label-free detection, promising to ease the time and cost burden of identifying and quantifying a vast number of molecular interactions in the era of “omics”.

The most widely used SPR setup is the Kretschmann configuration, in which a thin (~50 nm) layer of a noble metal (usually gold) is deposited on a glass substrate that is attached to a prism. The use of gold offers both convenience and limitations in the preparation of the sensing interface, which is a crucial part of biointeraction analysis.^{5,17} Current methods of functionalizing gold surfaces include a proprietary dextran matrix (Biacore chips) and self-assembled monolayers (SAMs) of thiols and disulfides. Commercial substrates with a carboxymethyl-dextran matrix have high immobilization capacity and reduced nonspecific adsorption versus bare gold;¹⁸ however, there is limited flexibility in chemical

- (3) Wang, S.; Boussaad, S.; Tao, N. J. In *Biomolecular Films*; Rusling, James F., Ed.; Marcel Dekker: New York, 2003.
- (4) Rich, R. L.; Myszka, D. G. *J. Mol. Recognit.* **2000**, *13*, 388–407.
- (5) Rich, R. L.; Myszka, D. G. *Curr. Opin. Biotechnol.* **2000**, *11*, 54–61.
- (6) Natsume, T.; Nakayama, H.; Janssen, O.; Isobe, T.; Takio, K.; Mikoshiba, K. *Anal. Chem.* **2000**, *72*, 4193–4198.
- (7) Caruso, F.; Jory, M. J.; Bradberry, G. W.; Sambles, J. R.; Furlong, D. J. *Appl. Phys.* **1998**, *83*, 1023–1028.
- (8) McDonnell, J. M.; Boussaad, S.; Pean, J.; Tao, N. J. *Anal. Chem.* **2000**, *72*, 222–226.
- (9) Sota, H.; Hasegawa, Y.; Iwakura, M. *Anal. Chem.* **1998**, *70*, 2019–2024.
- (10) Quinn, J. G.; O'Neill, S.; Doyle, A.; McAtamney, C.; Diamond, D.; MacCraith, B. D.; O'Kennedy, R. *Anal. Biochem.* **2000**, *281*, 135–143.
- (11) Rothenhausler, B.; Knoll, W. *Nature* **1988**, *332*, 615–617.
- (12) (a) Jordan, C. E.; Corn, R. M. *Anal. Chem.* **1997**, *69*, 1449–1456. (b) Smith, E. A.; Thomas, W. D.; Kiessling, L. L.; Corn, R. M. *J. Am. Chem. Soc.* **2003**, *125*, 6140–6148.
- (13) Kanda, V.; Kariuki, J. K.; Harrison, D. J.; McDermott, M. T. *Anal. Chem.* **2004**, *76*, 7257–7262.
- (14) Shumaker-Parry, J. S.; Zareie, M. H.; Aebbersold, R.; Campbell, C. T. *Anal. Chem.* **2004**, *76*, 918–929.
- (15) Lyon, L. A.; Musick, M. D.; Smith, P. C.; Reiss, B. D.; Pena, D. J.; Natan, M. J. *Sens. Actuators, B* **1999**, *54*, 118–124.
- (16) Wilkop, T.; Wang, Z.; Cheng, Q. *Langmuir* **2004**, *20*, 11141–11148.
- (17) Siegers, C.; Biesalski, M.; Haag, R. *Chem.—Eur. J.* **2004**, *10*, 2831–2838.

* Corresponding author. Phone (Quan “Jason” Chang): 951-827-2702. E-mail: quan.cheng@ucr.edu.

(1) Turner, A. P. F. *Science* **2000**, *290*, 1315–1317.

(2) Green, R. J.; Frazier, R. A.; Shakesheff, K. M.; Davies, M. C.; Roberts, C. J.; Tendler, S. J. B.; Homola, J. *Anal. Bioanal. Chem.* **2003**, *377*, 528–539.

functionalization of this matrix. The use of SAMs for surface modification has recently been reviewed by Whitesides et al.¹⁹ One of the common strategies for SPR chips is based on functionalization of SAMs of about 12 carbon length terminated with carboxylate,²⁰ amine,²¹ or ethylene glycol.^{22,23} Typically, the terminal groups are activated first, followed by covalent conjugation with capture molecules. The drawbacks of SAM methods include limited film stability, poor orientation/biocompatibility, and potential problems of protein adsorption and fouling. These limitations have necessitated alternative routes, such as use of cutinase substrates²⁴ and avidin/biotin coupling interactions.²⁵ Although the surface chemistry developed for gold has been of great value, the limitations of working on gold are becoming more noticeable with increasingly complex fabrication requirements for biomimetic systems and arrays. Improvements in materials and surfaces for broader capabilities in SPR spectroscopic analysis are urgently needed.

Glass is a standard material for biosensing in the planar format: inexpensive, widely used, and benefiting from a rich variety of well-developed attachment chemistries.^{26–28} Detection of DNA²⁹ and proteins³⁰ on glass substrates using microfluidic and fluorescence arrays is well-established. If the library of successful methods developed on glass could be applied to gold, many existing protocols and commercialized products could be transferred to SPR chips without the hurdle of adaptation. In fact, a number of strategies developed on glass have already been modified for use on gold, including antibody cross-linking, BSA blocking,^{31,32} nickel chelating attachment,³³ and tethered bilayers.³⁴ Adapting these methods to gold surfaces often proves to be a complex procedure, requiring time-consuming synthetic work to obtain suitable compounds and extensive manipulation of the existing protocols to be effective on the new surface.

An ideal way to simplify the process would be to coat the gold SPR substrate with glass (silicate) materials to achieve measurement directly on glass. Since the SPR signal decays exponentially

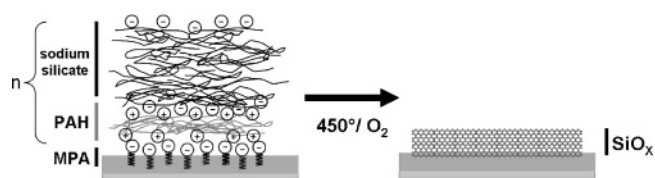


Figure 1. Cartoon presentation of the assembly process by LbL deposition of PAH and sodium silicate layers and calcination on the gold substrates.

within ~ 200 nm of the surface,³⁵ the coating must have a thickness on the order of nanometers to retain high detection sensitivity. Knoll and co-workers reported the use of a soft silicate (sol gel) coating on gold for SPR analysis, but “hard” glass surfaces prepared by chemical vapor deposition appear to have stability limitations in PBS buffer.³⁶ Recently, two independent reports showed a layer-by-layer (LbL) deposition method to form a sandwich structure of organic and inorganic layers on QCM crystals and silicon wafers.^{37–38} When the organic element is removed at high temperature, the film collapses to form a dense solid network of silicate.³⁷

In this work, we report the fabrication of stable silicate coatings of nanometer thickness on gold SPR substrates by an LbL/calcination process and demonstrate its utility in protein interaction analysis by SPR. The process of fabricating thin silicate layers on gold is illustrated in Figure 1. This glasslike structure on SPR substrates is expected to offer surface properties that are completely different from bare gold and to enable a host of new coupling chemistries for attachment. We chose to investigate supported bilayer membranes (SBMs), a lucrative application which has recently attracted great interest,^{39–41} and the molecular interactions (i.e., membrane-protein and receptor/ligand types) on these membranes by SPR. Supported membranes mimic cell membrane structure with the use of phospholipids via fusion of lipid vesicles on solid surfaces to form a bilayer membrane. It is important to note that lipid vesicles fuse readily on glass³⁹ and hydrophilic PDMS surfaces.⁴² Formation of a true bilayer membrane on gold, however, remains debatable. Long-chain alkanethiol SAMs have been used as the sublayer in the formation of hybrid bilayer membranes (HBMs).⁴³ However, this type of structure usually does not exhibit lateral fluidity and hinders the insertion of membrane biomolecules due to steric limitations.⁴⁴ To generate fluid membranes, polyion “cushions”⁴⁵ and tether strategies^{34,46} are typically used, which provide a hydrophilic “aqueous” layer between the SAM and the lipid membranes.

(18) Loefas, S.; Johnsson, B.; Tegendal, K.; Roennberg, I. *Colloids Surf., B* **1993**, *1*, 83–89.
 (19) Love, J. C.; Estroff, L. A.; Kriebel, J. K.; Nuzzo, R. G.; Whitesides, G. M. *Chem. Rev.* **2005**, *105*, 1103–1169.
 (20) Patel, N.; Davies, M. C.; Hartshorne, M.; Heaton, R. J.; Roberts, C. J. *Langmuir* **1997**, *13*, 6485–6490.
 (21) Wegner, G. J.; Lee, H. J.; Corn, R. M. *Anal. Chem.* **2002**, *74*, 5161–5168.
 (22) Mrksich, M.; Grunwell, J. R.; Whitesides, G. M. *J. Am. Chem. Soc.* **1995**, *117*, 12009–12010.
 (23) Houseman, B. T.; Gawalt, E. S.; Mrksich, M. *Langmuir* **2003**, *19*, 1522–1531.
 (24) Kwon, Y.; Han, Z.; Karatan, E.; Mrksich, M.; Kay, B. K. *Anal. Chem.* **2004**, *76*, 5713–5720.
 (25) Shumaker-Parry, J. S.; Aebersold, R.; Campbell, C. T. *Anal. Chem.* **2004**, *76*, 2071–2082.
 (26) Lee, S.-W.; Laibinis, P. E. *Biomaterials* **1998**, *19*, 1669–1675.
 (27) Yakovleva, J.; Davidsson, R.; Lobanova, A.; Bengtsson, M.; Eremin, S.; Laurell, T.; Emneus, J. *Anal. Chem.* **2002**, *74*, 2994–3004.
 (28) Sharma, S.; Desai, T. A. *J. Nanosci. Nanotechnol.* **2005**, *5*, 235–243.
 (29) Barinaga, M. *Science* **1991**, *253*, 1489.
 (30) Mitchell, P. *Nat. Biotechnol.* **2002**, *20*, 225–229.
 (31) MacBeath, G.; Schreiber, S. L. *Science* **2000**, *289*, 1760–1763.
 (32) Schweitzer, B.; Wiltshire, S.; Lambert, J.; O'Malley, S. O.; Kukanskis, K.; Zhu, Z.; Kingsmore, S. F.; Lizardi, P. M.; Ward, D. C. *Proc. Natl. Acad. Sci. U.S.A.* **2000**, *97*, 10113–10119.
 (33) Zhu, H.; Bilgin, M.; Bangham, R.; Hall, D.; Casamayor, A.; Bertone, P.; Lan, N.; Jansen, R.; Bidlingmaier, S.; Houfek, T.; Mitchell, T.; Miller, P.; Dean, R. A.; Gerstein, M.; Snyder, M. *Science* **2001**, *293*, 2101–2105.
 (34) Schiller, S. M.; Naumann, R.; Lovejoy, K.; Kunz, H.; Knoll, W. *Angew. Chem., Int. Ed.* **2003**, *42*, 208–211.

(35) Knoll, W. *Annu. Rev. Phys. Chem.* **1998**, *49*, 569–638.
 (36) Kambhampati, D. K.; Jakob, T. A. M.; Robertson, J. W.; Cai, M.; Pemberton, J. E.; Knoll, W. *Langmuir* **2001**, *17*, 1169–1175.
 (37) He, J.; Fujikawa, S.; Kunitake, T.; Nakao, A. *Chem. Mater.* **2003**, *15*, 3308–3313.
 (38) Cassagneau, T.; Caruso, F. *J. Am. Chem. Soc.* **2002**, *124*, 8172–8180.
 (39) Groves, J. T.; Ulman, N.; Boxer, S. G. *Science* **1997**, *275*, 651–653.
 (40) Tien, H. T.; Ottova, A. L. *J. Membr. Sci.* **2001**, *189*, 83–117.
 (41) Yang, T.; Baryshnikova, O. K.; Mao, H.; Holden, M. A.; Cremer, P. S. *J. Am. Chem. Soc.* **2003**, *125*, 4779–4784.
 (42) Phillips, K. S.; Cheng, Q. *Anal. Chem.* **2005**, *77*, 327–334.
 (43) Duschl, C.; Liley, M.; Corradin, G.; Vogel, H. *Biophys. J.* **1994**, *67*, 1229–1237.
 (44) Plant, A. L. *Langmuir* **1999**, *15*, 5128–5135.
 (45) Zhang, L.; Vidu, R.; Waring, A. J.; Lehrer, R. I.; Longo, M. L.; Stroeve, P. *Langmuir* **2002**, *18*, 1318–1331.
 (46) Stora, T.; Lakey, J. H.; Vogel, H. *Angew. Chem., Int. Ed.* **1999**, *38*, 389–392.

Supported bilayer membranes on PDMS microchips^{42,47} and glass slides⁴⁸ with low nonspecific interactions have been successfully demonstrated in protein analysis. These surfaces are mostly suitable for fluorescence measurements. In this paper, we will characterize the SBMs on gold substrates glassified with a silicate layer and demonstrate their use in the study of biotin/avidin interactions and detection of cholera toxin with ganglioside GM1 by surface plasmon resonance. Characterization of calcinated silicate layers by SEM and membrane lateral mobility by fluorescence recovery after photobleaching (FRAP) is carried out to probe the physical properties of the surface. Layer thickness change during LbL assembly and after calcination, membrane fusion, molecular binding, binding response reproducibility, and detection limits are determined with SPR. The advantage of using SBMs to minimize nonspecific adsorption of proteins on the silicate surfaces is also demonstrated and quantified.

EXPERIMENTAL SECTION

Materials and Instrumentation. Poly(allylamine hydrochloride) (PAH), avidin, bovine serum albumin (BSA), cholera toxin (CT), anti-CT IgG, and 3-mercaptopropionic acid (3-MPA) were obtained from Sigma-Aldrich. Sodium silicate was purchased from Fisher. Phosphatidylcholine (PC) and 1,2-dipalmitoyl-*sn*-glycero-3-phosphoethanolamine-*N*-(cap biotinyl) (PC-biotin) were from Avanti, 2-(12-(7-nitrobenz-2-oxa-1,3-diazol-4-yl)amino)dodecanoyl-1-hexadecanoyl-*sn*-glycero-3-phosphocholine (NBD-PC) was from Molecular Probes, and monosialoganglioside receptor (GM1) was from Matreya (Pleasant Gap, PA). Gold substrate fabrication in which a 46-nm thick gold layer is deposited by an e-beam evaporator onto the cleaned glass slides pretreated with mercaptoalkylsilane has been detailed in a previous report.¹⁶ A Biosuplar II instrument (Analytical μ -Systems, Germany) was used for all SPR experiments, whereas FRAP and fluorescence measurements were performed with a Meridian Insight confocal laser scanning microscope (CLSM) with argon laser excitation, cooled CCD, and 505-nm long-pass emission filter with a 40 \times /0.75 na Achromplan dipping objective.

Preparation of Ultrathin Silicate Layers. Cleaned gold substrates were immersed in 10 mM 3-MPA ethanol solution overnight, followed by extensive rinsing with ethanol and water. They were dipped into sodium silicate solutions (10, 20, and 40 g/L) for 2 min, followed by immersion in ultrapure water to rinse. They were dried in a nitrogen stream and dipped in PAH for 2 min, with subsequent rinsing and drying again. This process was repeated to build up the layers to the desired thickness while monitoring with SPR. The completed chips were then calcinated in a furnace by heating to 450 °C at a rate of 17 °C per min and allowing cooling to room temperature 4 h later. The thickness of the films was measured by SPR and calculated by fitting the data with the Sprangle program, which was kindly provided to us by Dr. Robert Corn at the University of California, Irvine.

Characterization of Calcinated Surfaces. Confocal and scanning electron microscopy (SEM) have been used for characterizing the calcinated chip surfaces to assess properties that may affect biosensor performance. SEM of the chips was obtained using a Philips XL30 FEG scanning electron microscope. Forma-

tion of lipid membranes was tested by exposing the surfaces to PC vesicles containing 2% NBD-PC for 1 h, followed by rinsing and imaging with the Meridian confocal microscope. The methods of vesicle preparation and FRAP with a CLSM have been previously reported.⁴² Protein adsorption was tested by injecting various concentrations of BSA, avidin, IgG, and CT in Tris buffer (10 mM with 150 mM NaCl, pH 7.4) over the calcinated chips and monitoring the change in the angle of minimum reflectivity.

SBM Biosensing on Ultrathin Silicate Layers. All responses were quantified by SPR using the "tracking" mode of angular scanning in a small range around the minimum angle. Vesicles of pure PC, 5 molar % PE-biotin/PC, and 5 molar % GM1/PC were prepared as previously reported.⁴³ The vesicles were injected into the SPR cell, and the flow was stopped for 1 h when the signal increase began to slow. The flow rate was then restored to 8.3 mL/h. After 10 min of rinsing to ensure the complete removal of free vesicles, the analytes were injected through a sample loop. When each binding assay was complete, the lipid membranes were removed with an injection of 5% Triton X-100 before repeating the experiment.

DISCUSSION

Layer-by-Layer Assembly of Polyelectrolyte Films on Gold.

LbL assembly of polyelectrolytes developed by Decher et al.⁴⁹ is known as an effective way to control the thickness of a film on a nanometer scale. We applied this method for the deposition of alternating layers of PAH and sodium silicate on gold, which showed regular growth in thickness. The deposition rate could be adjusted by a number of parameters. Figure 2 shows the effect of concentration, pH and the drying step on the assembly process. The uncertainty of the measurements due to removing and replacing the chips on the SPR was determined to be \sim 0.5 nm with a sample size of five measurements. The thickness of the polyelectrolyte layers was calculated by fitting to theoretical reflectivity curves from the Fresnel equations using an average refractive index (RI) of 1.455 for one PAH/silicate layer. This overall RI is based on a weighted combination of the RI for sodium silicate and PAH that assumes 40% hydration of PAH.⁵⁰ As shown in Figure 2a, increasing the concentration of sodium silicate increased the rate of growth. However, it should be noted that higher concentrations of sodium silicate, while giving rapid buildup, resulted in hazy or rough surfaces after several layers. On the basis of screening results with varied concentrations, a concentration range of about 10–40 g/L sodium silicate gave satisfactory growth rates while remaining free from visible surface defects and, thus, was used henceforth in this work.

Because the pH affects the forms of monomers in solution, it is a critical factor in controlling the morphology and thickness of the layers (Figure 2b). Although a pH value close to 8 gave the most rapid growth (\sim 1.3 nm/layer), layers made with solutions below pH 9 resulted in white films instead of smooth transparent layers. However, the growth rate at pH 10 was only \sim 0.7 nm/layer, almost half the rate at pH 8 (Figure 2b). A good compromise was found at pH 9.5, which allowed for marked growth and smooth deposition of the silicate layers. We also tested the effect of the drying process between rinse steps on the deposition rate (closed

(47) Phillips, K. S.; Dong, Y.; Carter, D.; Cheng, Q. *Anal. Chem.* **2005**, *77*, 2960–2965.

(48) Yang, T.; Jung, S. Y.; Mao, H.; Cremer, P. S. *Anal. Chem.* **2001**, *73*, 165.

(49) Decher, G.; Hong, J. D. *Ber. Bunsen-Ges. Phys. Chem.* **1991**, *95*, 1430.

(50) Zhang, L.; Longo, M. L.; Stroeve, P. *Langmuir* **2000**, *16*, 5093–5099.

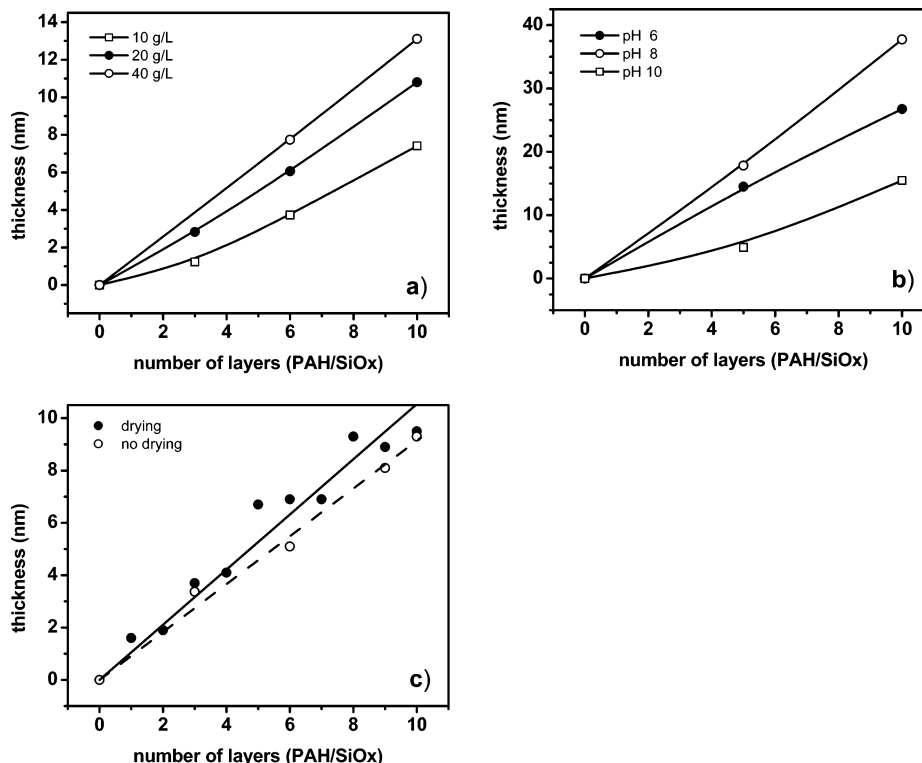


Figure 2. Effects of experimental parameters on the film thickness: (a) concentration of sodium silicate, (b) solution pH, and (c) drying process.

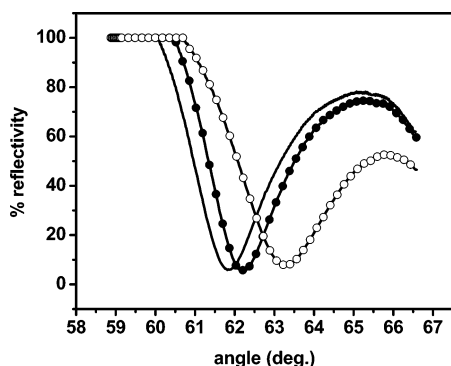


Figure 3. SPR reflectivity curves for a bare chip (smooth line), 10-layer PAH/silicate chip (open circles), and the calcinated chip (closed circles).

circles in Figure 2c). It was found that this process gave a growth rate similar to that of a continuous dipping method in which rinsing immediately precedes the next layer deposition without drying (open circles). The appearance of chips prepared using both ways was also similar. Since the process was performed manually, the slow transfer times necessitated a 2-min deposition time for each step to ensure good reproducibility. However, additional experiments indicated that even short, 30-s deposition times can provide similar growth rates.

Characterization of Calcinated Chips. After the chip was assembled by LbL deposition, it was then calcinated in a furnace to remove the organic layers and consolidate the silicate to form a solid structure. Figure 3 shows the reflectivity change in SPR measurements for a 10-layer assembly before and after calcination. To estimate the thickness of the silicate layer, a refractive index of 1.457³⁶ was used in the Fresnel calculations. We found that the reduction in thickness after calcination varied and appeared to

depend on the pH of the sodium silicate solution. For the chips deposited at pH 9–10, the average reduction in thickness was 59%, with the standard deviation being 17% ($n = 10$). In general, films that were thicker before calcination were found to reduce more after calcination. In cases in which precipitation occurred, calcination only led to a small reduction in thickness, providing a convenient means to screen out those chips which were unsuitable for SPR analysis.

Although SPR has subnanometer resolution for determination of thin-film thickness, it does not provide visual evidence of surface properties such as homogeneity and morphology. At present, imaging SPR also lacks the resolution needed to obtain fine structural detail. Therefore, SEM was used to characterize the calcinated surfaces at the micrometer and nanometer scale (Figure 4). From Figure 4, SEM reveals that the calcinated surfaces appear smooth at the micrometer scale, with sparsely spaced protrusions. At higher magnification, small cracks can be seen in the surface of a 1.9-nm silicate layer (the right image in Figure 4). These cracks were unexpectedly different from calcinated silicate layers prepared on silicon wafers, in which an AFM study revealed an RMS roughness of 0.8 nm,³⁷ indicating that the gold substrate may have a large impact on the silicate morphology. The width of these cracks ranges from 3 to 8 nm. Further characterization was carried out with fluorescence microscopy, showing that the spacing for the cracks agrees well with results from SEM images. As the silicate layer thickness increased, the crack and protrusion frequency decreased. When the thickness of the solid silicate film reached ~ 12 nm, it was possible to obtain highly homogeneous surfaces on which no cracks were observed with fluorescence microscopy. It is worth noting that despite the surface defects on ultrathin silicate layers, our studies with protein adsorption and binding response showed no major difference in performance for

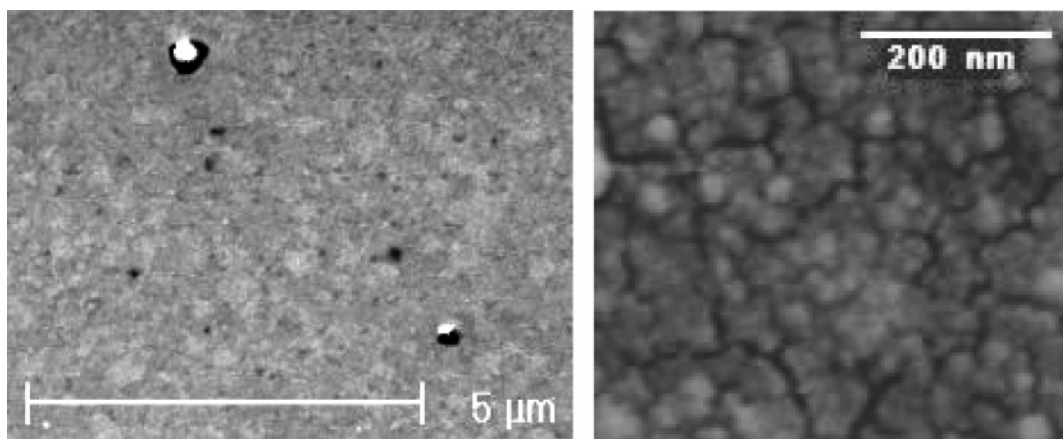


Figure 4. SEM images of the 1.9-nm calcinated silicate layer on gold substrate. Scale bar on the left is 5 μm , and the one on the right is 200 nm.

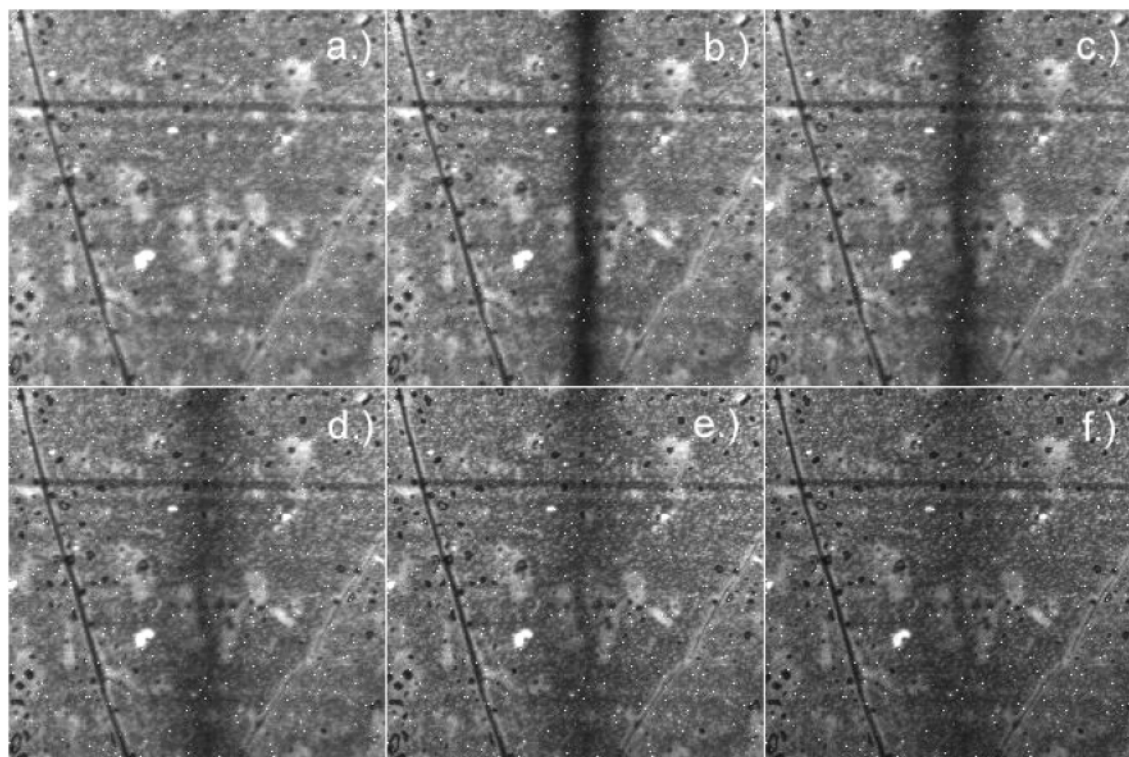


Figure 5. Fluorescent images of recovery after photobleaching of NBD-PC membranes on a 13.5-nm-thick silicate chip: (a–f) image before bleaching and 5, 10, 20, 30, and 45 s after bleaching.

the thin and thicker silicate layers after being covered with lipid membranes. Nevertheless, defects and rough areas of the surface may generate some unwanted effects on membrane properties and affect the long-term stability. Therefore, an effort is underway in our lab to use modified calcination conditions to obtain silicate surfaces <5 nm thick with few or no cracks or protrusions.

A key property for the silicate surface on gold substrates is whether it supports formation of a smooth and continuous membrane over a large area via vesicle fusion and if the structure on it shows intrinsic membrane properties, such as lateral mobility. FRAP is an effective method to characterize the mobility of the membranes. Figure 5 shows the FRAP results using a PC membrane on a 13.5-nm silicate-coated substrate. A uniform and continuous membrane is seen despite the presence of moderate surface features. After photobleaching, long-range lateral diffusion

of the membrane was observed, leading to a recovery pattern that fits well with the expected theoretical behavior. Using previously established methods,⁴² the data were fit to yield an average diffusion coefficient (D) of $1.4 \mu\text{m}^2/\text{s}$ and a mobile fraction close to unity. The D value obtained here is slightly low, but it is still in a reasonable range when compared with those obtained on glass and other substrates.^{51,52} Lipid membranes on the ultrathin (2–10 nm) silicate coatings were found to be continuous but slightly restricted, and FRAP experiments also revealed the occurrence of fluorescence recovery. Apparently, the smaller, nanoscale cracks did not appear to prevent formation of mobile SBMs on thin coatings. It is possible that the bilayers may extend

(51) Kalb, E.; Frey, S.; Tamm, L. K. *Biochim. Biophys. Acta* **1992**, *1103*, 307–316.

(52) Hovis, J. S.; Boxer, S. G. *Langmuir* **2001**, *17*, 3400–3405.

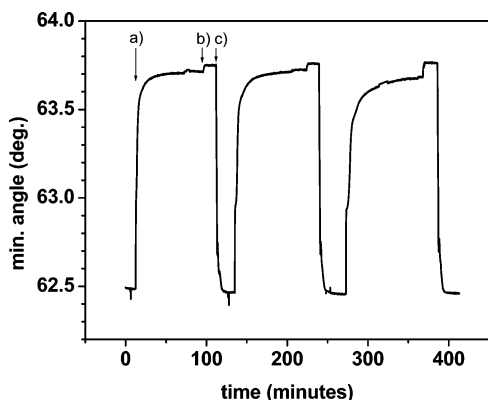


Figure 6. SPR sensorgram for the GM1-doped PC vesicles that shows membrane assembly, CT binding, and removal processes on the silicate surface: (a) injection of vesicles, (b) injection of CT, and (c) injection of 5% Triton. The concentration of CT used in the binding assays was 3.5, 3.5, and 8.5 $\mu\text{g/mL}$, respectively.

across these small cracks due to strong lateral interactions, resulting in the lateral mobility on imperfect surfaces. It is worth noting that the fluorescence signal on the ultrathin silicate/gold chips was quite dim, probably due to quenching via energy transfer to the underlying gold substrate.⁵³

To test the stability of the calcinated layers, the chips were incubated with Tris buffer for 3 h and then placed in the SPR flow cell. The minimum SPR angle was tracked over a period of 16 h, and the curves were compared with data obtained using bare gold chips. The minimum angle fluctuates about 0.01–0.02° over the 16-h period because of instrumental drift, but there was no major loss of material under normal operating conditions. The rugged stability of the silicate layers was further evidenced by the fact that the chips could be used for days in a flow cell with no changes observed in the signal response. After several days, the signal began to decrease because the gold started peeling from the glass slides due to pressure at the border of the Teflon flow cell gasket. We conclude that the adherence of the silicate layers to gold is strong, even stronger than that of gold to the mercaptosilane-modified glass substrate.

Protein Interaction Surface Study with SBMs on Silicate Layers by SPR. We then tested the formation and removal of SBMs on the silicate-coated gold chips. Figure 6 shows the effectiveness and reproducibility of the assembly of PC-GM1 membranes, CT binding, and cleaning of assembly structures with Triton X-100. After the vesicles were injected, the flow was stopped for 1 h to allow for vesicle fusion to occur on the silicate surfaces. The rate of increase in the minimum angle during the stopped flow period was sensitive to changes in the substrate surface and differences in vesicle composition. Binding measurement was carried out after thorough rinsing of the excess vesicles and stabilization of the signal. Interestingly, although the increase in the minimum angle caused by membrane assembly varied slightly between runs, it did not affect the reproducibility of binding. The average membrane thickness, calculated by using a refractive index of 1.45 for the lipid membrane,⁵⁴ was 4.2 ± 1.5 nm ($n = 12$) for PC, 4.7 ± 1.1 nm for PC-GM1 ($n = 16$), and 4.0 ± 0.7 nm for

PC-biotin ($n = 10$). These values are close to the expected value (4–5 nm) for the supported phospholipid bilayers. The nonionic surfactant Triton X-100 (5% v/v) was used to remove the whole membrane and bound proteins, a process which appeared to be highly effective (Figure 6). Sodium dodecyl sulfate (SDS) and ethanol were also tested, but only Triton removed the membrane reproducibly without a change in the baseline. When performing a large number of continuous experiments using this method with SPR, the loss of the binding signal was minimal, largely owing to the fresh surface generated each time the membrane was removed and reassembled. The ability to readily achieve a fresh surface is a highly desirable and attractive property for sensing interfaces and represents a marked advantage of silicate/SBM surface for SPR analysis. In comparison, the conventional strategy of regenerating a surface, which uses stripping buffers to remove antigens from surface bound antibodies, may cause irreversible denaturation and signal degradation with each successive run.

Protein adsorption was tested at two concentrations on the bare and SBM-functionalized calcinated chips (Figure 7). The 0.01 mg/mL concentration represents the high end of concentrations that might be tested in controlled experiments with only a few molecular species of interest. The 0.1 mg/mL concentration, on the other hand, represents an ideal concentration for total proteins found in diluted matrixes of body fluids and other samples used for biosensing. It was found that nonspecific adsorption of 0.01 mg/mL CT, BSA, and avidin on the calcinated chips resulted in a minute increase of 7, 5, and 8 millidegrees, respectively. This is almost a 10-fold improvement as compared to those on bare gold surfaces (52, 46, and 61 millidegrees). The same protein concentrations injected over calcinated surfaces with SBMs did not even result in a detectable minimum angle change. The minimum detectable signal change of the Biosuplar II SPR instrument used in this work was about 1–2 millidegrees, so the results suggest 30-fold or better reduction of protein adsorption on SBM coated silicate surfaces as compared to bare gold. The outstanding ability to prevent nonspecific adsorption allows for highly sensitive detection and effective discrimination of specific binding from nonspecific protein adsorption for SPR measurements and is critical for the validity of receptor/ligand screening, kinetics, and biomolecular interaction studies. The squelching of nonspecific adsorption at concentrations where specific binding coverage is nearly saturated likely indicates that the formation of SBMs is complete on the silicate surface, covering it quantitatively. As Figure 7 shows, a similar trend occurred when 0.1 mg/mL concentrations of the three proteins were injected over the chips, where the increase in minimum angle was many times greater for bare calcinated surfaces. At this concentration, the protein response on SBMs ranged from baseline to about 8 millidegrees, and the response on calcinated surfaces ranged from 11 to 61 millidegrees. Bare gold, on the other hand, resulted in 270, 135, and 456 millidegrees increases for CT, BSA, and avidin. Total protein concentrations of 0.1 mg/mL might be encountered when biosensing with diluted clinical or food/environmental samples. In this situation, because SPR is a label-free method, the signal from nonspecific binding of proteins other than the analyte of interest becomes a LOD-determining factor. Tests for adsorption of IgG yielded values similar to the three proteins above, with no detectable adsorption on membranes at the 0.01 mg/mL concen-

(53) Lakowicz, J. R. *Anal. Biochem.* **2001**, *298*, 1–24.

(54) Terrettaz, S.; Stora, T.; Duschl, C.; Vogel, H. *Langmuir* **1993**, *9*, 1361–1369.

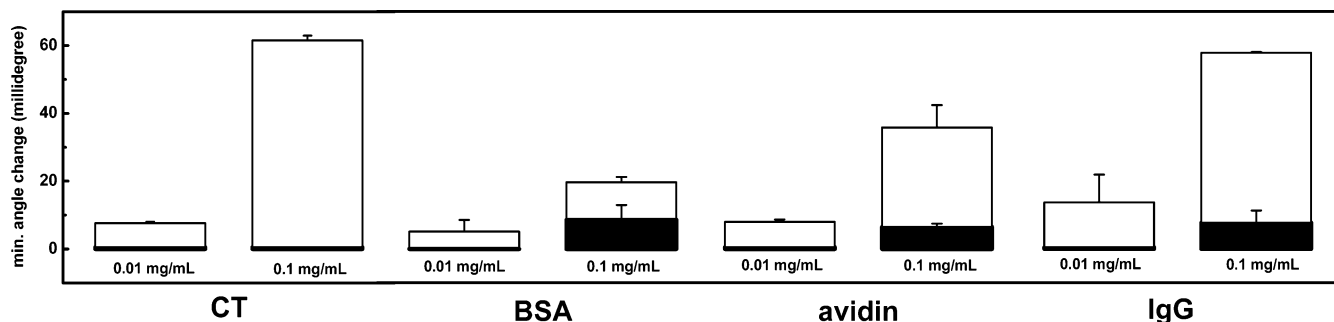


Figure 7. Protein adsorption of 0.01 and 0.1 mg/mL CT, BSA, avidin, and rabbit anti-CT IgG on bare silicate surface (white columns) and on a membrane-covered surface (black columns). The thick black lines at the base represent cases for which no signal could be discerned from noise.

tration level, as compared to a 13-millidegree increase on silicate and a 47 millidegree increase on gold. The results for 0.1 mg/mL IgG adsorption confirmed the substantial reduction in nonspecific protein adsorption on SBMs. An increase of 8 millidegree shift was obtained on SBMs, as compared to 50 millidegrees on calcinated surfaces and 317 millidegrees on bare gold. This is important because gold-conjugated antibodies are often used with SPR to amplify the signal from analyte binding.⁵⁵ If the nonspecific binding of these antibodies can be minimized, the signal-to-noise gain will be improved concurrently.

We tested two receptor/ligand systems with SBMs on the silicate/gold surface using SPR. The avidin/biotin interaction is a model system with very high binding affinity ($k_a = 10^{15} \text{ M}^{-1}$) and is increasingly being used to build sophisticated structures for enhanced detection strategies. The supported lipid membranes were prepared with PC vesicles doped with 5 mol % biotin-PE. As seen in Figure 8a, avidin bound strongly to the biotin-containing membranes with a linear relationship between response and concentration in the range of 1–6 $\mu\text{g/mL}$, corresponding to 15–90 nM. Considering the instrumental noise limitation of $\sim 0.001^\circ$, detection of proteins in the nanomolar concentration range shows the remarkable sensitivity of the SBM-coated silicate substrate. It is instructive to compare the nonspecific adsorption of avidin on the bare silicate surface to the signal from binding to biotin in the membrane. Figure 7 shows that adsorption of 10 $\mu\text{g/mL}$ avidin on the silicate-supported membranes was below the detection limit, and adsorption of 100 $\mu\text{g/mL}$ had a weak response of only 0.007° . The response for 6 $\mu\text{g/mL}$ avidin binding to the biotin functionalized membranes is $\sim 0.150^\circ$ (Figure 8a), giving a large, specific/nonspecific signal ratio. The results also give independent confirmation of our previous work using fluorescence assay,⁴² verifying that phospholipid membranes are highly effective to suppress nonspecific signal while retaining maximal binding response.

Another model system we tested on the silicate/gold substrates was cholera toxin detection with GM1. The purpose of using CT/GM1 is 2-fold: it is a well-characterized system, and cholera is a major health threat in countries with poor sanitation. The binding of CT to GM1 is similar to other protein toxins that bind to glycolipid receptors, such as botulinum neurotoxin (BT) and staphylococcus enterotoxin B (SEB), which can cause sickness and death in humans from food poisoning. The ganglioside GM1 was doped into vesicles (5 molar %) in a manner similar to that

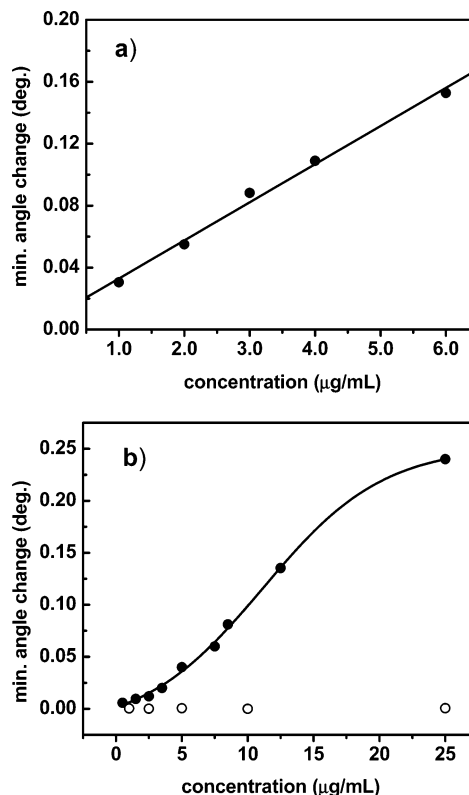


Figure 8. SPR biosensing response curves for proteins on the functionalized PC membranes assembled on calcinated silicate films: (a) biotin–avidin and (b) CT-GM1. The open circles in the CT-GM1 graph represent the control experiments in which CT was injected over PC membranes without GM1. A sigmoidal curve was used to help visualize the response for CT.

used for biotin-PE. The vesicles were then fused on the silicate surface, and a series of cholera toxin solutions of different concentrations were injected through the flow cell. The resulting standard curve is shown in Figure 8b. Reproducibility was calculated to be 7% RSD at a concentration of 3.5 $\mu\text{g/mL}$. Using the linear range of the lower portion of the curve, we obtained a LOD of 10 nM (0.85 $\mu\text{g/mL}$) for CT. In fact, as low as 0.5 $\mu\text{g/mL}$ CT solution could generate a distinguishable signal on this surface. Ultimately, to discuss the detection sensitivity of the SBM/silicate surface, the limitations of the instrument used in this work must be taken into account. High-end instruments such as the 2-channel Biacore systems have manifold better signal-to-noise performance than the SPR used in our lab due to proprietary microfluidic

(55) Lyon, L. A.; Musick, M. D.; Natan, M. J. *Anal. Chem.* **1998**, *70*, 5177.

systems and optics. Although it is difficult to directly compare the results with previous work, we found that Choi and co-workers reported a 2.5 $\mu\text{g}/\text{mL}$ LOD for botulinum neurotoxin with an antibody sandwich assay using the Biacore X instrument.⁵⁶ Another report showed a detection limit of 6 $\mu\text{g}/\text{mL}$ for *Escherichia coli* heat-labile enterotoxin by using GM1 and Spreeta.⁵⁷ From these results, it is clear that the use of SBMs on the silicate surface enables greater sensitivity than conventional systems while maintaining a high level of reproducibility. This surface allows the chip to be reused many times and minimizes nonspecific adsorption, and the use of SBMs displays receptors in a favorable orientation for protein capture. With the use of biotinylated antibodies and an intermediate layer of avidin, many proteins should be detectable on this surface.

CONCLUSIONS

We report the layer-by-layer fabrication of stable nanometer-scale silicate layers on gold SPR substrates and their use for biosensing of protein toxins. The LbL method of assembly is simple and inexpensive and allows for nanometer-scale control over film thickness. The rate of growth is tunable using several conditions, and the process should be amenable to large-scale production. SEM and fluorescence images show that ultrathin silicate surfaces have some protrusions and nanoscale cracks, which is different from the smooth surfaces obtained on silicon wafers.³⁷ The defects are likely due to the gold surfaces, different sodium silicate compositions, or calcination conditions. Nevertheless, the nanoscale cracks did not appear to affect the formation

of SBMs on the surface. In addition, it was possible to produce thicker silicate films in which no cracks were observed.

The properties of the supported bilayer membranes on the thin silicate layers were characterized by FRAP and SPR. The membranes are highly mobile, exhibiting great promise for membrane-associated biosensing applications. On these surfaces, there is low or no detectable signal from nonspecific adsorption of competing proteins with concentrations of 100-fold or more. This is crucial for SPR measurements because any molecules nonspecifically adsorbed to the surface will contribute to the overall signal. The limit of detection obtained in this work was 12–50-fold lower than other reports for detection of protein toxins with SPR. Since no incubation was used for ligand binding in the experiments, lower detection limits could be obtained by recirculating flow over a longer time period with a microfluidic apparatus.

In addition to the membrane-based protein analysis, we expect that the method reported here will inspire many other applications because the functionalization protocols for silicate/glass substrates and commercial reagents are readily available. Currently, we are exploring alternative silicate fabrication methods to generate surfaces that are stable, smooth on a larger scale, and possess highly protein-resistant properties.⁵⁸ The use of silicate on gold substrates frees SPR spectroscopic and imaging analysis from the limitations of thiol-based attachment chemistry, unfettering the method for a variety of new interfaces tailored to important applications in biosensing.

ACKNOWLEDGMENT

This work is supported in part by the National Science Foundation (BES-0428908). We thank Dr. Pingyun Feng and Xiqing Wang in the UCR Chemistry Department for help with the calcination process.

Received for review September 14, 2005. Accepted November 7, 2005.

AC051644Y

(56) Choi, K.; Seo, W.; Cha, S.; Choi, J. *J. Biochem. Mol. Biol.* **1998**, *31*, 101–105.

(57) Spangler, B. D.; Wilkinson, E. A.; Murphy, J. T.; Tyler, B. J. *Anal. Chim. Acta* **2001**, *444*, 149–161.

(58) After the completion of this manuscript, the work of Tawa and Morigaki came to our attention, in which a sputtering method was used to create a silicate surface on SPR gold substrates (Tawa, K.; Morigaki, K. *Biophys. J.* **2005**, *89*, 2750–2758). Vesicle fusion occurred readily on this surface, similar to the process observed on the calcinated surface we report here.